The Chemistry of a Dry Cloud: The Effects of Radiation and Turbulence

JORDI VILÀ-GUERAU DE ARELLANO

Department of Meteorology and Air Quality, Wageningen University, Wageningen, Netherlands

JOANNES W. M. CUIJPERS

KNMI, De Bilt, Netherlands

(Manuscript received 21 August 1998, in final form 8 July 1999)

ABSTRACT

The combined effect of ultraviolet radiation and turbulent mixing on chemistry in a cloud-topped boundary layer is investigated. The authors study a flow driven by longwave radiative cooling at cloud top. They consider a chemical cycle that is composed of a first-order reaction whose photodissociation rate depends on the cloud properties and time and a second-order chemical reaction between an abundant entrained reactant and a species with an initial concentration in the boundary layer. This turbulent reacting flow is represented numerically by means of a large eddy simulation. The simulation does not take evaporative cooling and aqueous-phase chemistry into account; that is, the authors simulate a dry smoke cloud.

The vertical concentration profiles of the reactants not in excess clearly show the appearance of gradients due to the chemical sources and sinks in the cloud. Moreover, the vertical-flux profiles depart from a linear profile. Fluxes that, in the absence of chemistry, are directed upward could change direction due to the different chemical reaction rate constants inside and below the cloud and because of the dominant downward motions generated by radiative cooling. The flux-budget analysis shows the relevance of the chemical term for the nonabundant species inside of the cloud. The exchange flux between the free troposphere and the boundary layer also depends on the chemical transformation above and in the cloud. An expression for the exchange velocity of reactive species is proposed in terms of an in-cloud flux, the production–depletion chemical rates, and the concentration jump at the inversion height. The calculated exchange velocity values for the smoke and the reactants differ considerably.

1. Introduction

In studies of atmospheric chemistry it is very important to determine the impact of boundary layer processes on chemical transformations. In particular, they could control the chemical reaction rates and could modify the spatial distribution and evolution of the reactants. The understanding and the quantification of these influences are needed in order to parameterize adequately the mixing and transport of reactants in large-scale models with complex chemical mechanisms. With regard to a dry convective boundary layer, previous studies (Schumann 1989; Gao and Wesely 1994; Sykes et al. 1994; Verver et al. 1997; Molemaker and Vilà-Guerau de Arellano 1998; Krol et al. 2000, hereafter KMV-G) have shown that the boundary layer turbulent structure exerts an influence on chemical reactions. The effect depends on several factors: the ratio of the turbulent timescale to the chemical timescale (Damköhler number), the concentration of species, and the way in which species are introduced into the boundary layer (Schumann 1989) and the chemical scheme (KMV-G).

In this study, the combined effect of cloud dynamics and the radiation field perturbed by the presence of a homogeneous cloud deck on chemistry is considered. Three main processes are considered. First, ultraviolet radiation is the driving mechanism that photodissociates key tropospheric species such as ozone or nitrogen dioxide. In contrast with the turbulent reacting flows studied in a dry convective boundary layer, the radiation field is strongly modified by cloud droplets and aerosols and as a consequence the photolysis coefficient is altered under cloudy conditions (Madronich 1987). Second, Donaldson and Hilst (1972) pointed to the importance of turbulent mixing in controlling the reaction rate of second-order chemical reactions. Some clouds (for instance, stratocumulus) are characterized by vigorous downward motions generated by sinking cold air, which produces a counterflow characterized by weak updrafts. This turbulent structure establishes separate reaction zones that might have different chemical reaction con-

Corresponding author address: Jordi Vilà-Guerau de Arellano, Department of Meteorology and Air Quality, Wageningen University, Duivendaal 2, 6701 AP Wageningen, Netherlands.
E-mail: jvila@hp1.met.wau.nl

© 2000 American Meteorological Society

Unauthenticated | Downloaded 05/08/21 11:21 AM UTC

stant rates. Third, the study of exchange of chemical species between the atmospheric boundary layer and the free troposphere is undertaken. This process depends on the longwave radiative cooling at the cloud top. The chemical transformation in the cloud could both enhance or diminish the value and the direction of this exchange flux.

The processes associated with clouds and atmospheric chemistry are complex and intrincate. In order to obtain worthwhile information, the scope of the investigation is framed in the following way. We consider only a radiatively active smoke cloud (dust cloud) (Bretherton et al. 1999) and neglect therefore the evaporation and condensation processes as well as aqueous-phase chemistry. Except for these latter processes, the situation closely resembles a marine homogeneous stratocumulus deck. Further, the chemical scheme under study contains three species that react in a cycle with first- and second-order reactions. The departure from chemical equilibrium of this cycle is studied in detail.

To investigate this turbulent reacting flow in a dry cloud, a large eddy simulation (LES) model is used. The LES is an appropriate tool to carry out this control case. It provides information on the spatial distribution and the statistics of the concentration fields, the fluxes, and covariances of the reactants. Moreover, the analysis of the LES results determine the main mechanisms that drive the reactants in the boundary layer. Measurements of the mean, variance, and covariance are scarce and often suffer from the fact that one or more of the reactants concentrations have values under the detection limit. In addition, it is also very difficult to obtain reliable fast response measurements to estimate the fluxes, variances, and covariances.

A brief description of the model and of the numerical simulation is explained in section 2. In section 3 the results are presented that include the overall statistics and the flux budget. Section 4 includes a discussion about the role of the chemistry on the exchange flux and its parameterization as a function of an exchange velocity. The conclusions are set forth in section 5.

2. Numerical simulation

a. Dynamics

The model used is the three-dimensional LES code developed and described in detail by Cuijpers and Duynkerke (1993) and Siebesma and Cuijpers (1995). Later modifications implemented in the LES model can be found in Cuijpers and Holtslag (1998). The model has been used for several intercomparisons of cloud studies (Moeng et al. 1996; Bretherton et al. 1999). The dynamics of the smoke convective boundary layer (SCBL) have been extensively described and discussed by Bretherton et al. (1999). Briefly, the turbulence of the SCBL is driven by the cloud-top radiative cooling of a chemically inert scalar (smoke) that has been uniformly distributed throughout the boundary layer. Similar to vanZanten et al. (1999), the longwave radiative flux is prescribed by a linear function with a radiative forcing equal to 60 W m^{-2}. The initial cooling rate is about 4 K h^{-1}. The depth of the radiative flux divergence is about 50 m into the cloud. The surface buoyancy flux and the smoke flux are zero. Large-scale forcing (subsidence) is put to zero. Cloud-top cooling rates are comparable to the ones observed in marine stratocumulus. During the simulation the cloud-top height increases with time. Water phase changes are not taken into account, that is, evaporative cooling is omitted.

The simulation covers a 3-h period and the statistics presented in the following section were obtained by averaging over the last hour. Variables between brackets are volume averaged over the whole SCBL. The horizontal domain is 3200 m $\times$ 3200 m (64 $\times$ 64 grid points). The domain height is 1280 m, which is solved with 128 grid points. The 10-m vertical grid is the minimum length to accurate simulate processes near the inversion (vanZanten et al. 1999; Stevens and Bretherton 1999). The time step of the simulation is 0.5 s.

b. Chemistry

A chemical module is included for studying the effects of ultraviolet radiation and turbulence on chemistry. With regard to the chemical species, the space discretization for the advection term (limited $\kappa = \frac{1}{3}$ scheme) (Vreugdenhil and Koren 1993) and diffusion term is the same as the one used for the other scalar variables and it is applied to the conservation equation of the newly implemented chemical species. However, for the time discretization the leapfrog scheme has been substituted by the two-stage Runge–Kutta time discretization, which retains the positivity property of the κ scheme (Hundsdorfer et al. 1993).

The chemical term in the conservation equation of the reactants is solved using an explicit method that also preserves positiveness, the so-called two-step solver (Verwer 1994). Sandu et al. (1997) compared this solver with other explicit chemical solvers and concluded that the two-step method is the one that gives the best performance.

After these modifications, any chemical scheme can be used in conjunction with the current LES model. However, in this study, the following generic reactions are taken into account:

$$A \xrightarrow{j} B + C \tag{1}$$

$$B + C \xrightarrow{k} A. \tag{2}$$

Reaction (1) is photolyzed at a reaction rate constant j (s^{-1}) which is a function of the cloud properties, cloud height, date, and time. Reaction (2) has the reaction rate k ($ppb^{-1}\ s^{-1}$). These two reactions allow us to study the effect of the different production and depletion rates and the shift on the chemical balance because of the

Unauthenticated | Downloaded 05/08/21 11:21 AM UTC

influence of the boundary layer processes. Following the analysis used by KMV-G, the subgrid effects of the chemical terms are omitted.

Initially, species A and B have the same concentration and vertical profile as the smoke (concentration equal to 1 ppb in the entire SCBL, $z < 700$ m, and 0 ppb above the boundary layer, $z > 700$ m). Species C is entrained at the top of the SCBL. Its concentration above the layer is 30 ppb and in the SCBL it is 20 ppb. These conditions are very common in chemical systems, where one species is normally more abundant than the other reactants. No emission or dry deposition processes (surface fluxes) are taken into account.

Although the SCBL turbulent characteristics are closer to those of a nighttime stratocumulus situation (turbulence is driven only by longwave radiative cooling), the radiative part of the chemical cycle [reaction (1)] is driven by ultraviolet radiation, that is, diurnal conditions. In consequence, the simulation of this idealized case enables us to study the main atmospheric physical processes that cause the chemical cycle to depart from the equilibrium state and the consequences of this departure.

The presence of clouds dramatically modifies the UV radiation field (Madronich 1987; van Weele and Duynkerke 1993; Vilà-Guerau de Arellano et al. 1994). This disturbance is included in the LES by means of a parameterization. The variation with height and time of the photolysis rate constant j is taken into account using

$$j(z, t) = a_1(z) \exp\left\{a_2(z)\left[1 - \frac{1}{\cos(a_3(z)\theta_s(t))}\right]\right\}. \quad (3)$$

The j parameterization is calculated by solving the radiative transfer equations by means of the discrete ordinate method and by fitting the solution to the expression (3) (Krol and van Weele 1997). The coefficients a_1, a_2, and a_3 are functions of height and they depend on the chemical reaction, the cloud location and thickness, and the cloud optical depth. The day and time dependence is included in the solar zenith angle θ_s. The coefficients of the photolysis rates [expression (3)] are determined assuming a cloud base fixed at $z = 500$ m. The values of j are dependent on the deepening of the boundary layer depth and consequently the coefficients of (3) are updated according to this growth, that is, boundary layer depth varies with time. The cloud optical depth is constant and equal to 20. The ultraviolet surface albedo is 0.05. The geographical and time dependence of the photolysis rate constants are set to those at a latitude 23.45° and longitude 0° for the Julian day 172 and fixed to the maximum value of 1200 UTC, that is, solar zenith angle is 0. This value is kept constant during the simulation.

The selected chemical species photolyzed is NO_2 (species A). Consequently, reaction (3) involves the formation of NO_2 via the oxidation of NO (species B) by O_3 (species C) at a chemical reaction rate $k = 4.75 \times 10^{-4}$ (ppb s)$^{-1}$. Figure 1 shows the various profiles of the photolysis rate used during the whole simulation. The scattered diffusive radiation in the cloud leads to a linear increase in the photodissociation rates with a maximum just below cloud top (Madronich 1987). The figure shows the rise of this maximum following the deepening of the cloud top. In the subcloud layer the j vertical profile is almost constant with height, but it has lower values than the ones calculated in clear sky under otherwise similar conditions.

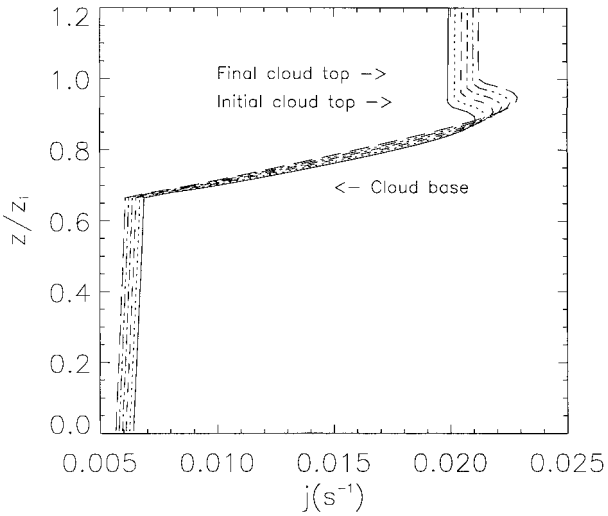

FIG. 1. Evolution of the photodissociation rate j [reaction (1)] vertical profile from the beginning to the end of the simulation. The j parameterization is a function of the SCBL deepening.

3. Simulation results

The following sections present the results of the turbulent reacting SCBL and discuss the implications of radiation and turbulent mixing for chemical cycles that occur in the presence of clouds. As Moeng (1986) and Duynkerke et al. (1995) mentioned, the statistics in cloudy boundary layers show a large variation and depend on the cloud properties and on the heat and moisture fluxes at the surface. Similarly, the statistics of chemical species depend largely on the internal chemical sources and sinks, on the initial concentrations, and on the Damköhler number [the ratio of the turbulent timescale to the chemical timescale, as defined in Molemaker and Vilà-Guerau de Arellano (1998)]. Despite the difficulty with finding universal scaling parameters, we have attempted to generalize the numerical results, and consequently all the figures are presented in a nondimensional way. The dynamic scaling parameters used are the convective velocity scale w_* (Deardorff 1980; Nicholls and Leighton 1986) and the one-hour averaged (between hour 2 and 3) boundary layer depth z_i. This depth is defined as the height of the isosurface where the smoke concentration equals 0.5, horizontally averaged over all columns. For the smoke and the reactants

Unauthenticated | Downloaded 05/08/21 11:21 AM UTC

TABLE 1. Corresponding scaling parameters and other relevant variables of the turbulent-reacting smoke cloud boundary layer. The values between brackets are volume-averaged values in the SCBL that have been averaged in the last hour of the simulation (between hour 2 and 3).

z_i	744 (m)
w_*	8.6 10^{-1} (m s^{-1})
$\langle \text{TKE} \rangle^{1/2}$	7.8 10^{-1} (m s^{-1})
$\langle w'\theta' \rangle$	1.0 10^{-2} (K m s^{-1})
$\langle S \rangle$	9.40 10^{-1} (ppb)
$\langle A \rangle$	1.01 (ppb)
$\langle B \rangle$	8.60 10^{-1} (ppb)
$\langle C \rangle$	2.04 10^{1} (ppb)
S_*	2.0 10^{-3} (ppb)
A_*	1.6 10^{-2} (ppb)
B_*	1.1 10^{-2} (ppb)
C_*	3.5 10^{-2} (ppb)
D_A	8.3
D_B	8.4
D_C	3.5 10^{-1}

the following scaling parameters are used: the volume-averaged concentration $\langle \chi \rangle$ and a concentration scale χ_* defined as

$$\chi_* = \frac{1}{z_i w_*} \left| \int_0^{z_i} \overline{w'\chi'}\, dz \right|, \tag{4}$$

where $\overline{w'\chi'}$ is the turbulent flux. Cuijpers and Holtslag (1998) proposed a similar expression, but without the absolute value of the integral, to calculate the nonlocal fluxes.

Table 1 summarizes the scaling parameters and the most characteristic numbers calculated from variables averaged in time over the last hour of the simulation. Variables between brackets are volume averaged and with an overbar are slab averaged over horizontal planes. The prime ($'$) is used to indicate the deviation from the slab-averaged value. These parameters will be discussed in detail and will be used in the following sections. It is important to note that neither the dynamical flow (the SCBL grows steadily due to cloud-top radiative cooling) nor the chemical system (the photolysis rate is dependent on height and time) reaches a stationary state. However, it is shown in section 4 that a quasi-steady situation is attained before the LES simulation statistics are calculated.

a. Vertical profiles of the concentrations

The vertical profiles of the smoke concentration and the species *A* concentration are plotted in Fig. 2. The radiatively active smoke is well mixed in the entire SCBL and the profile agrees well with the values presented in the intercomparison paper (Bretherton et al. 1999).

The vertical concentration profile of species *A* shows two distinct regions: the cloud layer and the subcloud layer. In the first region, a strong negative concentration gradient is created in the whole cloud. This is because

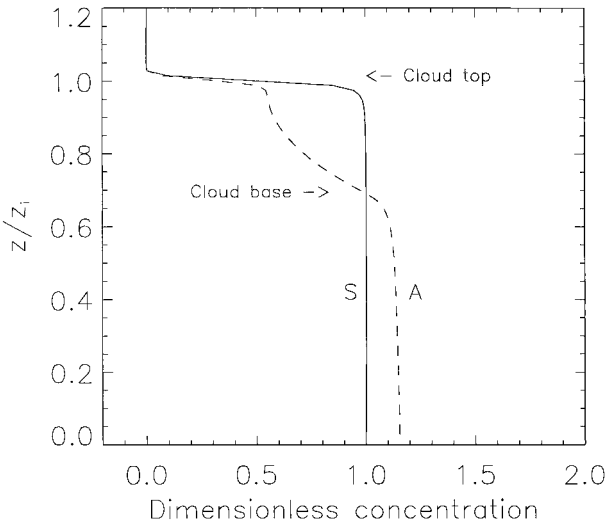

FIG. 2. Averaged vertical profile of the smoke concentration (continuous line) and of the species *A* concentration (dashed line). The values are made dimensionless by the respective volume-averaged concentration. The averaging period corresponds to the last hour of the 3-h simulation.

of the almost linear increase of the photolysis rate in the cloud. In the subcloud layer, the concentration decreases slightly with height. An explanation of this decrease is given in the discussion of Fig. 4.

Figure 3 shows the vertical profiles of the two species that react with the second-order chemical reaction. The profile of species *B* shows a pattern opposite to the profile of species *A*. The concentration has its maximum value (1.5 times larger concentration than in the subcloud layer) at the top. Below the cloud, a slight increase with height in the concentration is observed. In order to check the consistency of the calculations, the vertical

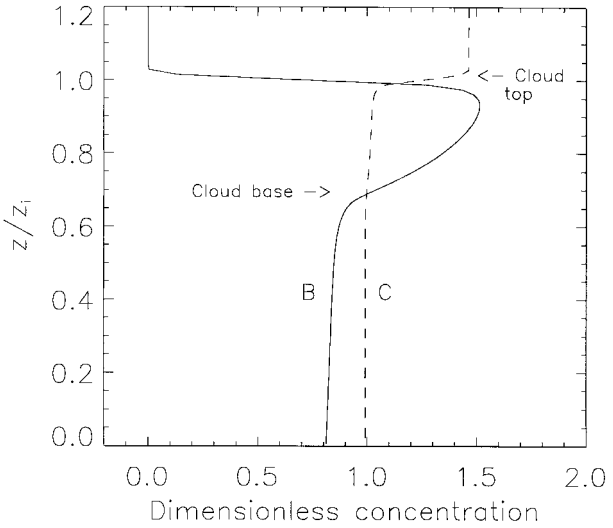

FIG. 3. As in Fig. 2, but for the concentration of species *B* (continuous line) and the concentration of species *C* (dashed line).

Unauthenticated | Downloaded 05/08/21 11:21 AM UTC

profile of the nondimensional chemically inert species $A + B$ has also been computed (not plotted). The vertical profile matches the inert smoke profile.

The entrained species C shows a well-mixed profile. This reactant is the most abundant in the simulation. Species with lower concentrations (A and B in our case) are much more sensitive to the effect of radiation and turbulent mixing on chemistry, and in addition both species limit, because of their low concentrations, the chemical system performance.

We can determine which species can be more influenced by the boundary layer processes calculating the ratio of the turbulent timescale to the chemical timescale, the so-called Damköhler number (D_i). The Damköhler numbers of the two species are defined:

$$\langle D_A \rangle = \frac{z_i}{w_*} j, \qquad \langle D_B \rangle = \frac{z_i}{w_*} k \langle C \rangle. \tag{5}$$

Table 1 shows these numbers for the current simulations. For species A and B, $\langle D_A \rangle$, $\langle D_B \rangle > 1$. The order of magnitude of these numbers indicates that the concentration and fluxes of the mentioned species can be largely influenced by the chemical term in their respective governing equations.

The chemical production and depletion rates in the SCBL can be mapped by calculating the instantaneous photostationary-state relation:

$$\phi = \frac{kBC}{jA}, \tag{6}$$

where A, B, and C are the instantaneous concentrations.

If $\phi = 1$, chemical production and depletion rates are equal, that is, the chemical cycle is in equilibrium. In our simulation, deviations from this equilibrium are due to the effects of boundary layer processes on the chemistry: photolysis dependent on height due to the radiation perturbation by the cloud, and the amplifications of concentration fluctuations because of the second-order chemical reactions. If $\phi > 1$, species A is produced and species B and C are depleted and vice versa. Figure 4 shows an instantaneous vertical cross section of the vertical velocity (w) and ϕ. In the cloud layer ($0.67 < z/z_i < 1$), one can distinguish a clear spatial distribution of ϕ. Regions dominated by the sinking cold air ($w < 0$) have values of ϕ larger than one and with maximum values in the core of the downdrafts (higher than 1.4). In the upper part of this region, species B, which is transported by the updraft and chemically produced at cloud top, gets into the downdraft and mixes with species C, which is entrained from the inversion layer. Thereafter, both species are carried down and they react. An explanation of this departure from chemical equilibrium is given below. At cloud top, the reactants contained in an air parcel are in chemical balance ($\phi = 1$). The downward motion moves the air parcel to a lower height where the j values are smaller. The transport and the mixing timescales are faster than the timescale of the chemical system to reach a new chemical equilibrium. As a consequence, departures of ϕ, $\phi > 1$, are found in the core of the downdrafts. A similar explanation but opposite behavior, $\phi < 1$, is found for the air parcels transported from the subcloud layer into the cloud.

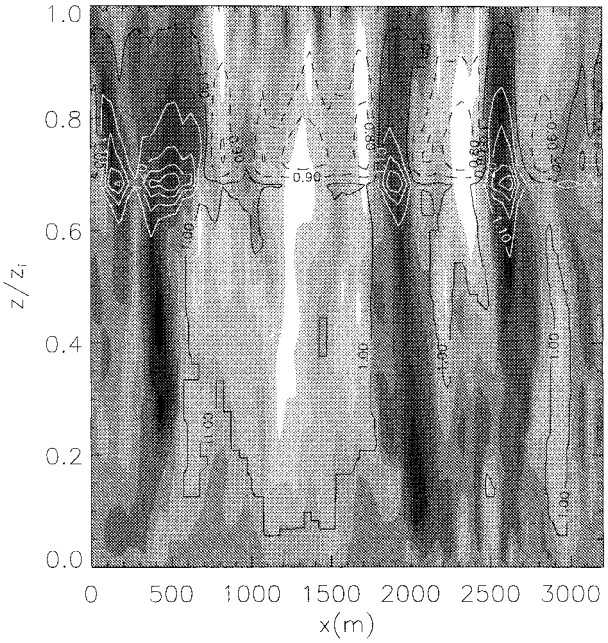

FIG. 4. Instantaneous vertical cross section of the vertical velocity and photostationary-state relation taken at the end of the simulation. The vertical velocity color palette ranges from a minimum value of -1.3 m s^{-1} (black) to a maximum value of 0.98 m s^{-1} (white). Continuous and white lines indicate $\phi > 1$ and dashed and black lines indicate $\phi < 1$. The ϕ contour interval is 0.1.

In the subcloud layer ($z/z_i < 0.67$), we found that the photostationary state has still values larger than one in the regions dominated by the downdraft. However, the values are closer to 1 compared to the ones of the cloud layer. This shows that under conditions where the photolysis rate is constant with height (such as the subcloud layer, see Fig. 1) and at regions with an efficient mixing the chemical cycle is closer to chemical equilibrium. In the areas with positive vertical velocity, the inefficient mixing of species B and C yields values of ϕ smaller than one, but also closer to the equilibrium value. Regions characterized by updraft motions occupied larger areas in the SCBL compared to the downdraft regions. As was previously stated, the chemical activity depends closely on the mixing of reactants. This is the reason for the slight decrease with height of the species A concentration observed in the subloud layer (see Fig. 2). Opposite behavior holds for species B.

Figure 5 shows the averaged photostationary-state relationship [Eq. (6)]. The largest departure from equilibrium is found near cloud base. In this transition layer between the subcloud and the cloud, the j values vary from an almost constant value to j values that increase

Unauthenticated | Downloaded 05/08/21 11:21 AM UTC

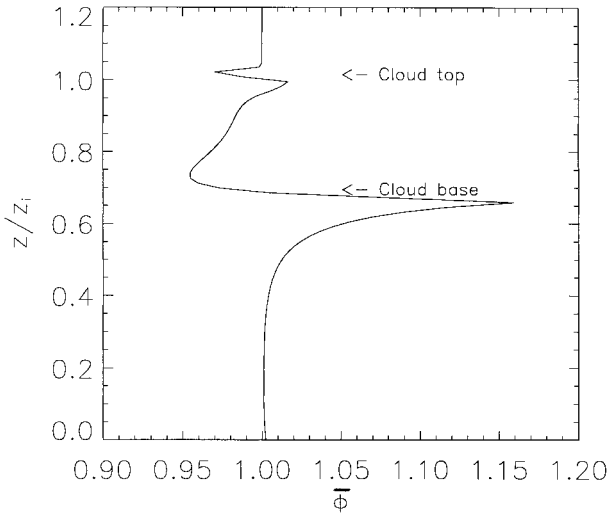

FIG. 5. Averaged vertical profile of the photostationary-state relation (ϕ).

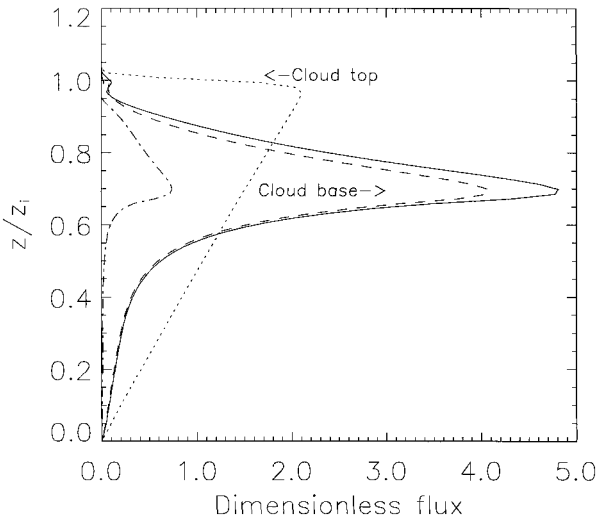

FIG. 6. Averaged vertical profile of the smoke flux (dotted line) and reactant *A* flux (continuous line). The dashed line is the resolvable flux of *A* and the dashed-dotted line is the subgrid contribution to the flux of species *A*. The values are made dimensionless by the convective velocity scale (w_*) and the volume-averaged concentration scale (χ_*). The averaging period corresponds to the last hour of the 3-h simulation.

with height. The maximum value $\phi = 1.16$ can be explained by the transport, in the downdrafts, of the reactants that are out of a chemical balance (see Fig. 4). In the cloud, the values smaller than 1 show that larger regions are occupied by the updrafts where turbulent mixing is less active and in consequence the depletion rate of species *A* is higher than the production rate ($\phi < 1$). The linear increase of $\overline{\phi}$ in the cloud clearly follows the *j* profile. At cloud top, the maximum value of $\overline{\phi}$ is due to the *j* maximum (see Fig. 1). Note that van Weele and Duynkerke (1993) estimated, using aircraft measurements, the vertical variation of $\overline{\phi}$ in a cloudy boundary layer and they found a similar pattern with the distinct behavior between the cloud and subcloud layer. Our numerical simulation corroborate their finding and adds new information on the horizontal variation of the photostationary state due to the SCBL turbulent structure.

These numerical results also suggest that deviations from the chemical equilibrium are not only produced by other chemical reactions competing with (1) and (2) (Cantrell et al. 1993), but also by the variation with height of the photolysis rate and the heterogeneous mixing produced by the turbulent structure of the SCBL. The chemical system under study requires several minutes to recover the chemical balance. Turbulent fluctuations and radiation alterations have a similar timescale. In consequence, the chemical cycle is always out of balance in the cloud because of the concentration spatial distribution created by the different chemical reaction rate constants inside the cloud.

b. Vertical profiles of the fluxes

Figure 6 shows the vertical-flux profile of the smoke flux and the flux of reactant *A*. For the latter species, the resolvable, the subgrid components, and the sum of both components are shown. The flux values are normalized by $w_*\chi_*$. As was found in the intercomparison study (Bretherton et al. 1999), the smoke flux increases linearly from zero at the surface to a maximum value close to the top of the SCBL and sharply decreases to zero at the inversion.

In the absence of chemical reactions, species *A* and *B* would each have had a profile similar to that of the smoke-flux profile, that is, an upward flux in the whole SCBL with a maximum value below the boundary layer height. The high nonlinearity of the flux profile for species *A* is due to the chemical sources and sinks inside the cloud. A positive flux is found in the whole cloud with a maximum value at cloud base. In the subcloud layer, the vertical-flux profile has smaller values than the inert smoke flux. The prescription of deposition and emission fluxes could alter the flux profiles in the subcloud layer.

Figure 7 shows the dimensionless vertical profile of the reactant flux of species *B*. For this reactant, one can also observe the effect of the different location and rates of the chemical sources and sinks on the flux profile. At cloud top, $z/z_i > 0.9$, and due to the highest production of species *B* (highest photolysis rate of species *A*), an upward-dimensional flux is found. Therefore, a certain amount of species *B* produced at this level is detrained from the SCBL and the exchange flux is enhanced by the chemical production at cloud top (see section 4). However, at lower heights and in the bulk of the cloud, the flux of species *B* is directed toward the surface. The reason is the transport of species *B* in the downdraft and its depletion reaction with species *C*. Similar to the flux profile for *A*, the minimum value is

Unauthenticated | Downloaded 05/08/21 11:21 AM UTC

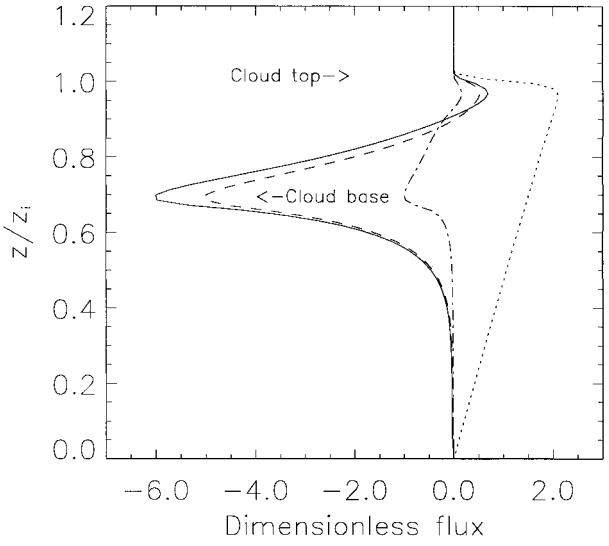

FIG. 7. As in Fig. 6, but for the flux of species *B*.

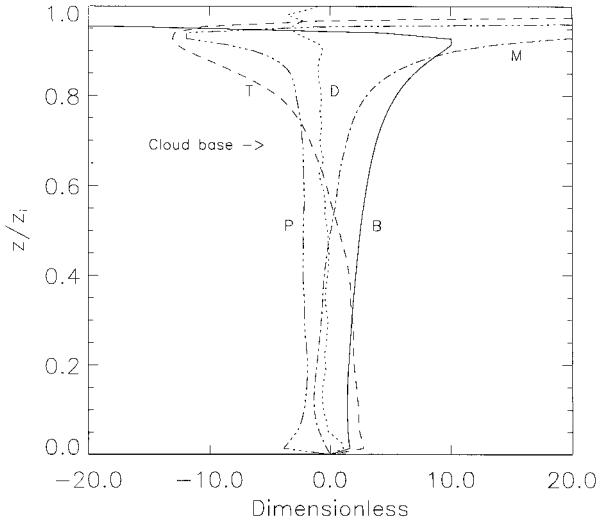

FIG. 8. Budget of the resolvable-scale smoke flux. The values are made dimensionless by the factor $w_*^2\chi_*/z_i$. The letter stands for the following terms: buoyancy (B), dissipation (D), pressure-scalar covariance (P), mean gradient (M) and turbulent transport (T).

found at cloud base. In the subcloud layer, $z/z_i < 0.67$, the flux profile rapidly tends to zero with decreasing height.

Similar to the concentration profile of the inert $A + B$ species, the dimensionless flux profile of $A + B$ has an identical profile as the smoke flux (not shown).

c. Flux budgets

In order to determine the role of the chemical term in the vertical-flux profile, the flux budget of the resolvable scale for the smoke is calculated and compared later on with the flux budget of reactant *B*.

Assuming horizontal homogeneity, one can find an expression for the smoke vertical-flux budget of the resolvable-scale $\overline{w's'}$,

$$\underbrace{\frac{\partial\overline{w's'}}{\partial t}}_{\text{I}} = \underbrace{\frac{g}{\Theta_o}\overline{\theta's'}}_{\text{B}} - \underbrace{\overline{w'^2}\frac{\partial\overline{S}}{\partial z}}_{\text{M}} - \underbrace{\frac{\partial\overline{w'^2s'}}{\partial z}}_{\text{T}} - \underbrace{\overline{s'\frac{\partial\pi}{\partial z}}}_{\text{P}} - \underbrace{\left\{\overline{s'\frac{\partial\tau'_{3j}}{\partial x_j}} + \overline{w'\frac{\partial(S'_s)_j}{\partial x_j}}\right\}}_{\text{D}}, \quad (7)$$

where w', s', and θ' are the fluctuating components of the vertical velocity, the concentration, and the temperature, respectively. Here Θ_o is a reference state potential temperature, $\overline{S}$ is the slab-averaged concentration, and π is a modified pressure defined as $[(p - p_o)/\rho_o] + (\frac{2}{3})E$, where p is the pressure, p_o and ρ_o are a reference density and a reference pressure, and E is the subgrid turbulent kinetic energy. Finally, the subgrid-scale stress for momentum and scalar are represented by τ'_{3j} and $(S'_s)_j$. The term on the left-hand side is the imbalance (I) due to nonstationarity. The right-hand side consists of the following terms: buoyancy (B), mean gradient (M), turbulent transport (T), pressure-scalar covariance (P), and dissipation (D) (interaction between resolved and subgrid-scale components). This last term has two contributions: subgrid-scale kinetic energy and subgrid-scale fluxes (S'_s). Figure 8 shows the right-hand terms of Eq. (7) made nondimensional by $w_*^2\chi_*/z_i$. In the bulk of the cloud, the buoyancy and the mean-gradient terms are the production terms that are balanced by the turbulent transport term and the pressure covariance term. The turbulent transport term becomes a gain term in the subcloud layer. The flux budget presented here agrees very well with the one calculated by Cuijpers and Holtslag (1998) for a similar simulation of the SCBL (Fig. 3d in their paper).

Figure 9 shows the flux-budget terms for reactant *B*. An additional term due to the chemical activity (CH) appears now in the flux-budget equation (7). The term CH reads

$$CH = j\overline{wA} - k\overline{wBC} = j\overline{w'a'} - k(\overline{B}\,\overline{w'c'} + \overline{C}\,\overline{w'b'} + \overline{w'b'c'}). \quad (8)$$

Note that in (8) the subgrid-scale contributions of the chemistry are omitted. Compared to Fig. 8, the main gain term is the chemical one and the main loss term is the mean gradient term. A similar flux budget, but opposite sign in the chemistry and mean-gradient terms, holds for species *A*. The departure from chemical equilibrium in the cloud leads to the formation of the gradient concentration. The maximum (minimum) value of the flux for species *A* (*B*) in Figs. 6 and 7 is because of the significant contribution of the chemical term in Eq. (7). This budget analysis stresses the important role

Unauthenticated | Downloaded 05/08/21 11:21 AM UTC

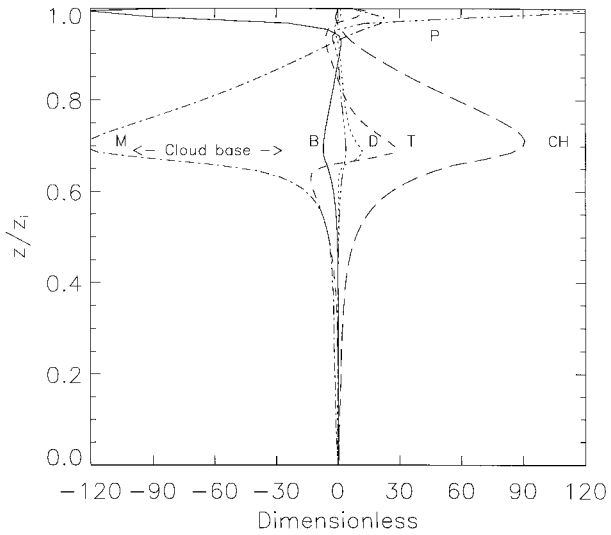

FIG. 9. As in Fig. 8, but for species *B*. The chemical component of the budget flux is indicated with a CH.

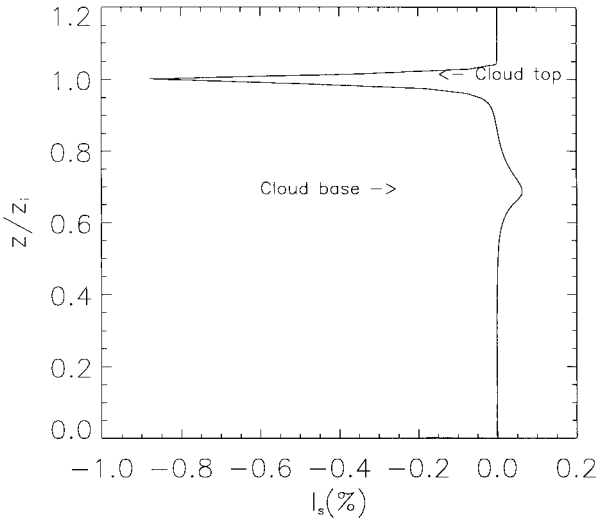

FIG. 10. Averaged vertical profile of the intensity of segregation for species *B* and *C*.

of the chemical term in the governing equations of reacting flows where the chemistry is unable to reach an equilibrium.

It is important to mention that the chemical term in the flux-budget equation differs from the chemical term in the concentration equation. From (8), one can write a horizontally averaged photostationary-state relation for the flux, $\overline{\phi}_f$ as

$$\overline{\phi}_f = \frac{k\overline{wBC}}{j\overline{wA}}. \tag{9}$$

Note that although chemical equilibrium can be reached for the concentration variables, that is, $\overline{\phi} = 1$, the chemical term in the flux-budget equation can be still significant, that is, $\overline{\phi}_f \neq 1$, since it depends not only on the concentration but also on the turbulent fluxes of the species. However, in the case under study and as Figs. 4, 5, and 9 show, $\overline{\phi}$ and $\overline{\phi}_f$ are always different from 1 in the cloud.

It is important to point out once again that the effect of the chemical term is larger in the case of species that are less abundant and have higher Damköhler numbers (such as species *A* and *B* in this study) and in the regions where chemical activity is more relevant. The vertical-flux profile of the abundant species *C* (not plotted) corroborates this explanation since departures from the linearity are less evident than for species *A* and *B*, and in consequence the CH term in the flux-budget equation is much smaller.

d. Intensity of segregation

Another relevant second moment for chemically reactive species is the covariance between two reactants. This variable is generally normalized by the product of the volume-averaged concentrations, namely, the intensity of segregation (I_s) (Schumann 1989), which reads for the second-order chemical reaction

$$I_s = \frac{\overline{b'c'}}{\overline{B}\,\overline{C}}. \tag{10}$$

A positive value of I_s (positive covariance) indicates that species are transported together (premixed situation). Here $I_s = 0$ corresponds to the situation when species are uniformly mixed. As a consequence, the rate of the chemical term in the averaged concentration equation will be enhanced by the extra contribution of the small-scale concentration fluctuations and the reaction will proceed faster than the product of the average concentrations. If $I_s < 0$, species are segregated (negative correlation) and therefore reaction rates are retarded because of the inefficient mixing. Large negative values of I_s were found in the studies of the dry convective boundary layer. As was mentioned in the introduction, all these studies were based on an irreversible second-order chemical reaction. Here, the intensity of segregation is analyzed for a closed chemical system, that is, chemical cycle.

Figure 10 shows the vertical profile of the I_s (as a percentage) of species *B* and *C*. As Schumann (1989) concluded in his paper, low values of the intensity of segregation are to be expected due to the high concentration ratio of the species *B* and *C*, in our simulation $\langle C\rangle/\langle B\rangle \approx 24$. In addition, the inclusion of the backward reaction [reaction (1)] also tends to decrease the absolute value of I_s (KMV-G).

The vertical profile also reveals the change of sign in the covariance. At cloud top, the negative value (and absolute maximum) indicates a region where species *B* transported by the updrafts mixes and reacts with the entrained air rich of species *C*, that is, negative correlation. In the lower part of the cloud ($z/z_i < 0.8$), re-

Unauthenticated | Downloaded 05/08/21 11:21 AM UTC

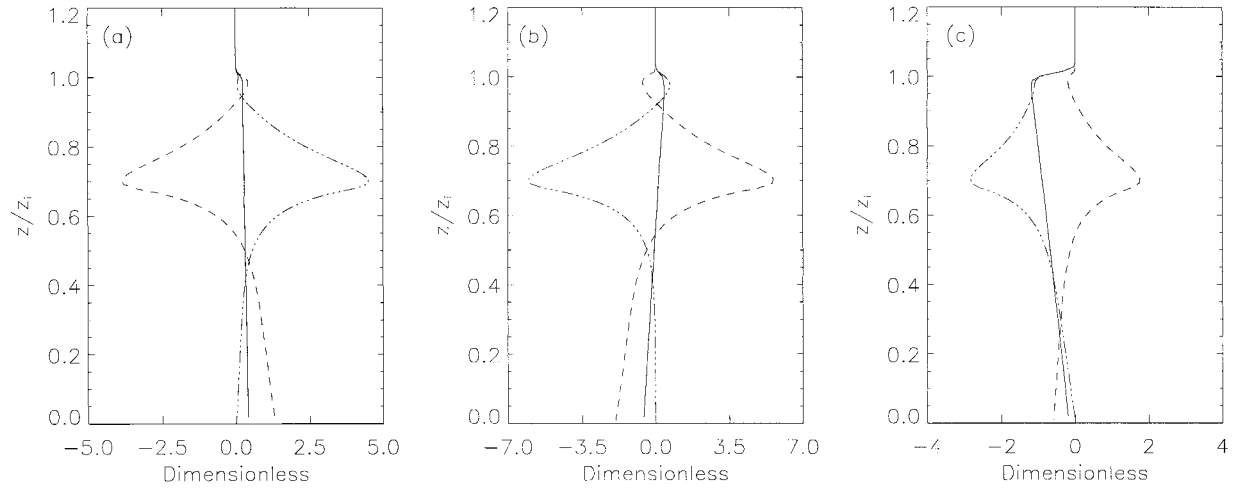

FIG. 11. Averaged vertical profile of the *total* flux (F_t) (continuous line), flux (dashed-dotted line), and and chemical term (dashed line) for (a) reactant *A*, (b) reactant *B*, and (c) reactant *C* which are the three terms of expression (14), respectively. The terms are made nondimensional by the factor $w_*\chi_*$.

action (1) produces species *B* and *C*, which are transported together toward the surface, that is, positive correlation. This yields small but positive value for I_s. In conclusion, the I_s sign is closely related to the transport of species in the SCBL. Finally, one notes that the I_s results differ from the dry CBL with a bottom-up and top-down species (Schumann 1989; Molemaker and Vilà-Guerau de Arellano 1998) where the I_s vertical profile is always negative in the entire boundary layer.

4. Exchange rate

At the inversion, the mixing of species from the free troposphere into the boundary layer (and vice versa) is an important process that mesoscale and large-scale models need to account for adequately. In this section, an expression to estimate the exchange (entrainment or detrainment) flux of the reactants is derived, which explicitly includes the chemical transformation of the species. The derivation is included below.

The horizontally averaged equation for the concentration reads

$$\frac{\partial \overline{C}}{\partial t} = -\frac{\partial \overline{w'c'}}{\partial z} + \overline{R}, \tag{11}$$

where the three terms are the rate of change of the concentration, the turbulent transport term, and the chemical term, respectively. In order to investigate whether the simulated flux is in a quasi-steady state, one can take the vertical gradient of (11), which yields

$$\frac{\partial}{\partial t}\left(\frac{\partial \overline{C}}{\partial z}\right) = -\frac{\partial^2 \overline{w'c'}}{\partial z^2} + \frac{\partial \overline{R}}{\partial z}. \tag{12}$$

The quasi-steady assumption of this equation implies that the lhs term of this equation is negligible compared with the rhs terms, that is, $(\partial/\partial t)(\partial \overline{C}/\partial z) \approx 0$. Consequently, and under this assumption, if one integrates twice (12), the result for the lhs is a linear profile.

With regard to the rhs, one can define the *total* flux (F_t) as the sum of the turbulent flux of the reactant (first term) plus the integral of the chemical term (second term),

$$F_t = -\int\int \frac{\partial^2 \overline{w'c'}}{\partial z^2}\, dz^2 + \int\int \frac{\partial \overline{R}}{\partial z}\, dz^2$$
$$= -[\overline{w'c'}]_z^{H_+} + \int_z^{H_+} \overline{R}\, dz, \tag{13}$$

where the integration limits are an arbitrary value in the SCBL (z) and a level above the boundary layer (H_+). The turbulent flux ($\overline{w'c'}(H_+)$) above the inversion is neglectable compared to the other terms of (13). As a consequence, Eq. (13) can be written as

$$F_t(z) = \overline{w'c'}(z) + \int_z^{H_+} \overline{R}_i\, dz. \tag{14}$$

Figure 11 shows the three terms of expression (14) for the three reactants. The terms have been made dimensionless by $w_*\chi_*$. A linear profile of F_t is found in the whole boundary layer for the three species. In agreement with Fig. 9, this result indicates the importance to account for the chemical term when chemistry departs from an equilibrium.

In the cloud, and particularly for species *A* and *B*, the turbulent flux and the chemical term are much larger than F_t. In consequence, for species *A* and *B*, the *total* flux depends largely on the balance of the two rhs of (14). Species *C* has a very similar profile, but with opposite sign, to the smoke. This indicates that, at cloud top, the chemical term plays a minor role compared to the turbulent-flux term.

From the total-flux profile one can attempt to estimate

Unauthenticated | Downloaded 05/08/21 11:21 AM UTC

TABLE 2. The F_t, the concentration jump $\Delta\overline{C}$, and the exchange velocities for the smoke and for the reactants. The averaged values correspond to the last hour of the simulation (between hours 2 and 3).

Species	F_t (ppb m s^{-1})	$\Delta\overline{C}$ (ppb)	w_{ex} (m s^{-1})
Smoke	3.61×10^{-3}	-8.73×10^{-1}	4.13×10^{-3}
A	3.66×10^{-3}	-5.62×10^{-1}	6.51×10^{-3}
B	3.58×10^{-3}	-1.19	3.01×10^{-3}
C	-3.63×10^{-2}	8.48	4.28×10^{-3}

the values of the exchange velocity for the three reactants. The exchange of species between the inversion layer and the boundary layer can be related to the total flux F_t, the concentration jump between both layers ($\Delta\overline{C}$) and an exchange velocity (w_{ex}). The concentration jump is defined as the $\overline{C}$ just above (H_+) and the $\overline{C}$ just below the inversion (H_-), that is, a height close to the cloud top. Therefore, integrating (11) over an assumed discontinuous inversion, defined by the upper limit $H_+ = H + \epsilon$ and by the lower limit $H_- = H - \epsilon$, and letting $\epsilon \to 0$ results in

$$F_t = - w_{ex}\Delta\overline{C}. \tag{15}$$

Combining (14) and (15), and after discretizing the integral chemical term, one can calculate the exchange velocities for the reactants at the interface of the boundary layer and the inversion

$$w_{ex} = \frac{-1}{\Delta\overline{C}}\left[\overline{w'c'}(H_-) + \sum_{i=H_-}^{H_+} \overline{R}_i \Delta z\right], \tag{16}$$

where the index i indicates the level height near H_- and H_+, respectively. From (16) it is clear that if the photostationary state holds, $\phi = 1$, at the inversion, w_{ex} will have the same value for the smoke and the three reactants. Table 2 shows the exchange velocities for the smoke and the three reactants. The values of the total flux and the concentration jump have also been included. For the same period, the value of the inversion growing rate $w_i = dh/dt$ is 3.87×10^{-3} m s^{-1}. Before analyzing the exchange velocity results, it is worth mentioning possible error sources in the determination of these values for inert species. Here vanZanten et al. (1999) have pointed out that it is more appropriate to calculate the exchange velocities assuming a finite inversion thickness instead of a discontinuous inversion. The numerical solution of the governing equations can also introduce errors in the estimation of w_{ex}.

With regard the w_{ex} values for the reactants, the similarity of the exchange velocities values for the smoke and for the reactant *C* shows that the latter species is acting almost as an inert scalar because it has a large concentration compared to the other two species. The exchange velocities for the inert species $A + B$ and $A + C$ should be independent of the chemistry. One can calculate these w_{ex} from Table 2. The values are almost equal to w_{ex} for the smoke.

For reactants *A* and *B*, the exchange velocity clearly departs from the smoke value. Note that initially both species have the same profile as the smoke. In consequence, and in absence of chemistry, they would have had equal exchange velocities. The largest w_{ex} value corresponds to reactant *A* due to its highest depletion rate near cloud top, which produces a considerable decrease of the concentration jump at the inversion. An opposite behavior is found for reactant *B*, which has the smallest value for the exchange velocity due to the chemical production and its relative low concentration compared to species *C*. In conclusion, it is shown that the total flux that includes the turbulent flux and the chemical term is the appropriate flux to estimate the exchange velocities. These velocities are very sensitive to the chemical activity near cloud top, which can produce large variations in the concentration jump. Additionally, it is important to mention that the inclusion of the chemical term on (16) is analogous to the correction due to the chemical transformation for the parameterization of the dry deposition of the reactants (Fitzjarrald and Lenschow 1983; Galmarini et al. 1997).

5. Conclusions

The combined effect of ultraviolet radiation and turbulent mixing appears to have a large influence on the concentration fields and the fluxes of chemically reactive species. A numerical representation of a chemically active dry cloud (no evaporative cooling, no aqueous-phase chemistry) has been studied by means of a large eddy simulation (LES). The smoke convective boundary layer (SCBL) is driven from the top through radiative cooling of a chemically inert smoke. The chemistry cycle is formed by three species that react with a first- (species *A*) and a second-order chemical reaction (species *B* and *C*). Species *C* is entrained at the inversion height and has a much larger concentration in the SCBL than species *A* and *B*. The latter two and the inert smoke have the same initial conditions, the concentration is one in the SCBL and zero above this region. The surface flux is zero for smoke and the three reactants. Species *A* is photodissociated with a rate that depends on the cloud properties, the deepening of the SCBL, the ultraviolet surface albedo, and the time. The photodissociation rate has been calculated assuming that the cloud has an optical depth of 20 and is located in the upper part of the SCBL. As a consequence, for the chemistry, two vertical layers have been clearly established: a cloud layer and a subcloud layer.

The vertical concentration profiles of the less abundant species *A* and *B* depend strongly on the location and on the rate variation of the chemical sources and sinks. In particular, a maximum of the concentration of species *B* is found at the cloud top due to the largest depletion of the photolyzed species *A*. This reactant shows a strong vertical negative gradient inside the cloud. These results indicate that cloud chemistry models that assumed that the species are homogeneously

Unauthenticated | Downloaded 05/08/21 11:21 AM UTC

mixed might produce large errors and have to account for the spatial, both horizontal and vertical, variations of the reaction rate constants.

The photostationary-state relation ϕ, a ratio of the production and depletion rates of the two chemical reactions, shows a large horizontal and vertical variability in the SCBL. In the cloud layer, the downdrafts are characterized by ϕ values larger than one. The most effective mixing between the newly formed species *B* and the entrained species *C* makes the second-order chemical reaction become more active that the photolysis rate. Opposite behavior is found in the upward motions that clearly show values of ϕ smaller than one. In the subcloud layer, the chemical equilibrium is almost established in the downdraft and updraft motions. It is in this region where the chemical cycle has enough time to reach a balance.

The flux profiles for the reacting *A* and *B* species are strongly influenced by chemical transformation and they clearly depart from the linear profile of the chemically inert smoke. Absolute maximum (minimum) values are found for species *A* (and *B*) at the cloud base. In absence of surface fluxes, the vertical fluxes of species *A* and *B* in the subcloud layer rapidly tend to zero. The changes in the slopes of the flux profile for the abundant species *C* appears to be less sensitive to the chemistry. The budget of the resolvable scale of the flux for species *B* shows that the chemical term becomes the major source term that balances the loss by the shear term. For Damköhler numbers close to one and nonabundant species, this implies that the chemical term in the flux-budget equation should be taken explicitly into account in higher-order closure models and flux parameterizations when the chemistry is out of balance due to the atmospheric processes.

A parameterization is proposed for the exchange flux between the SCBL and the inversion layer. The exchange flux has two components: the in-cloud turbulent flux and the chemical production–depletion rates above and below the inversion height. The exchange velocities of the three reactants calculated by means of the LES differ from each other and from the velocity calculated for the chemically inert smoke. The values are very sensitive to the concentration jump between the SCBL and the free atmosphere. The exchange velocity for species *A* is the largest due to the highest photolysis rate (depletion) at cloud top. In contrast, the chemical production has a tendency to diminish the exchange velocity of species *B*.

It is important to mention that in the absence of reliable and complete measurements of chemically active species, the numerical results obtained with the LES make it an appropriate model for studying and analyzing key features of reactants in various types of atmospheric boundary layers. However, further studies should be addressed to more complex cases and to make use of previous (Paluch et al. 1995) or future cloud chemistry studies based on observational data.

Acknowledgments. Both authors acknowledge the NATO collaborative research Grant CRG 970040 to sponsor the respective research visits. The authors would like to thank Peter Duynkerke for valuable discussions relating to this work. Stefano Galmarini, Maarten Krol, Jan Matthijsen, and Margreet van Zanten gave enlighting suggestions on an early version of the manuscript. Maarten Krol kindly provided the parameterization of the photodissociation rate.

REFERENCES

Bretherton, C. S., and Coauthors, 1999: An intercomparison of radiatively-driven entrainment and turbulence in a smoke cloud, as simulated by different numerical models. *Quart. J. Roy. Meteor. Soc.*, **125,** 391–425.

Cantrell, C. A., and Coauthors, 1993: Peroxy radicals as measures in ROSE and estimated from photostationary state deviations. *J. Geophys. Res.,* **98,** 18 355–18 366.

Cuijpers, J. W. M., and P. G. Duynkerke, 1993: Large eddy simulations of trade wind with cumulus clouds. *J. Atmos. Sci.,* **50,** 3894–3908.

——, and A. A. M. Holtslag, 1998: Impact of skewness and nonlocal effects on scalar and buoyancy fluxes in convective boundary layers. *J. Atmos. Sci.,* **55,** 151–162.

Deardorff, J. W., 1980: Cloud-top entrainment instability. *J. Atmos. Sci.,* **37,** 131–147.

Donaldson, C. P., and G. Hilst, 1972: Effect of inhomogeneous mixing on atmospheric photochemical reactions. *Environ. Sci. Technol.,* **6,** 813–816.

Duynkerke, P. G., H. Zhang, and P. J. Jonker, 1995: Microphysical and turbulent structure of nocturnal stratocumulus as observed during ASTEX. *J. Atmos. Sci.,* **52,** 2763–2777.

Fitzjarrald, D. R., and D. H. Lenschow, 1983: Mean concentration and flux profiles for chemically reactive species in the atmospheric surface layer. *Atmos. Environ.,* **17,** 2505–2512.

Galmarini, S., J. Vilà-Guerau de Arellano, and J. Duyzer, 1997: Flux of chemically reactive species inferred from mean concentration measurements. *Atmos. Environ.,* **31,** 2371–2374.

Gao, W., and M. L. Wesely, 1994: Numerical modelling of the turbulent fluxes of chemically reactive trace gases in the atmospheric boundary layer. *J. Appl. Meteor.,* **33,** 835–847.

Hundsdorfer, W. H., B. Koren, M. van Loon, and J. G. Verwer, 1993: A positive finite-difference advection scheme applied on locally refined grids. International CWI Rep. NM-R9309, CWI, Netherlands.

Krol, M. C., and M. van Weele, 1997: Implications of variations in photodissociation rates for global tropospheric chemistry. *Atmos. Environ.,* **31,** 1257–1273.

——, M. J. Molemaker, and J. Vilà-Guerau de Arellano, 2000: Photochemistry in the convective boundary layer. *J. Geophys. Res.,* in press.

Madronich, S., 1987: Photodissociation in the atmosphere: 1. Actinic fluxes and the effects of ground reflections and clouds. *J. Geophys. Res.,* **92,** 9740–9752.

Moeng, C. H., 1986: Large-eddy simulation of a stratus-topped boundary layer. Part I: Structure and budgets. *J. Atmos. Sci.,* **43,** 2886–2900.

——, and Coauthors, 1996: Simulation of a stratocumulus-topped planetary boundary layer: Intercomparison among different numerical codes. *Bull. Amer. Meteor. Soc.,* **77,** 261–277.

Molemaker, M. J., and J. Vilà-Guerau de Arellano, 1998: Turbulent control of chemical reactions in the convective boundary layer. *J. Atmos. Sci.,* **55,** 568–579.

Nicholls, S., and J. Leighton, 1986: An observation study of the structure of stratiform cloud sheets: Part I. Structure. *Quart. J. Roy. Meteor. Soc.,* **112,** 431–460.

Paluch, I. R., S. McKeen, D. H. Lenschow, R. D. Schillawski, and

Unauthenticated | Downloaded 05/08/21 11:21 AM UTC

G. L. Kok, 1995: Evolution of the subtropical marine boundary layer: Photochemical ozone loss. *J. Atmos. Sci.*, **52,** 2967–2976.

Sandu, A., J. G. Verwer, M. van Loon, G. R. Carmichaels, F. A. Potra, D. Dabdub, and J. H. Seinfeld, 1997: Benchmarking stiff code solvers for atmospheric chemistry problems: i. Implicit vs explicit. *Atmos. Environ.,* **31,** 3151–3166.

Schumann, U., 1989: Large-eddy simulation of turbulent diffusion with chemical reactions in the convective boundary layer. *Atmos. Environ.,* **23,** 1713–1729.

Siebesma, A. P., and J. W. M. Cuijpers, 1995: Evaluation of parametric assumptions for shallow cumulus convection. *J. Atmos. Sci.*, **52,** 650–666.

Stevens, D. E., and C. S. Bretherton, 1999: Effects of grid resolution on large-eddy simulation of radiatively driven entrainment through a strong inversion. *Quart. J. Roy. Meteor. Soc.*, **125,** 425–441.

Sykes, R. I., S. F. Parker, D. S. Henn, and W. S. Lewellen, 1994: Turbulent mixing with chemical reactions in the planetary boundary layer. *J. Appl. Meteor.*, **33,** 825–834.

van Weele, M., and P. G. Duynkerke, 1993: Effects of clouds on the photodissociation of NO_2: Observations and modelling. *J. Atmos. Chem.*, **16,** 231–255.

vanZanten, M. C., P. G. Duynkerke, and J. W. M. Cuijpers, 1999: Entrainment parameterization in convective boundary layers derived from large eddy simulations. *J. Atmos. Sci.*, **56,** 813–828.

Verwer, J. G., 1994: Gauss seidel iterations for stiff codes from chemical kinetics. *SIAM J. Sci. Comput.*, **15,** 1243–1250.

——, H. van Dop, and A. A. M. Holtslag, 1997: Turbulent mixing of reactive gases in the convective boundary layer. *Bound.-Layer Meteor.*, **85,** 197–222.

Vilà-Guerau de Arellano, J., and J. Lelieveld, 1998: Chemistry in the atmospheric boundary layer. *Clear and Cloudy Boundary Layers,* A. A. M Holtslag and P. G. Duynkerke, Eds., Royal Netherlands Academy of Science and Arts, 267–286.

——, P. G. Duynkerke, and M. van Weele, 1994: Tethered-balloon measurements of actinic flux in a cloud-capped marine boundary layer. *J. Geophys. Res.*, **99** (D2), 3699–3705.

Vreugdenhil, C. B., and B. Koren, 1993: *Notes on Numerical Fluid Mechanics. Numerical Methods for Advection-Diffusion.* Vieweg, 373 pp.

Unauthenticated | Downloaded 05/08/21 11:21 AM UTC